ULTRASOUND IMAGING FOR IDENTIFYING DYNAMICS OF SOFT TISSUE

Daisuke Yamada[⋆†] *Alperen Degirmenci*[⋆] *Robert D. Howe*[⋆]

[⋆] John A. Paulson School of Engineering and Applied Sciences,
Harvard University, Cambridge, MA 02138
[†] Toyota Research Institute North America, Ann Arbor, MI 48105

ABSTRACT

This paper describes the development of a non-invasive system for characterizing tissue dynamics. The system combines medical ultrasound imaging with an optical tracking system and a vertical exciter that can impart whole-body vibrations on seated subjects. Tissue motion was extracted from the ultrasound images, and in combination with the optical tracker data, the frequency response of the tissue was calculated based on the commanded vibration of the seat and the resultant motion of the tissue. Dynamics of abdominal organs and the upper leg were characterized using the developed system. The ultrasound imaging method presented here will provide insight into the dynamics of soft tissues, as well as their boundary conditions with surrounding organ systems. The identified characteristics can be utilized for surgical planning and simulation as well as for validating a finite element model that is being developed to predict vehicular ride comfort in the early stages of automobile design.

Index Terms— Ultrasound, tracking, tissue dynamics

1. INTRODUCTION

Understanding the *in vivo* dynamics of soft tissue, including its interaction with adjacent tissues, is a key problem for many fields, because it is expected to improve fidelity of computational models of human body. In the preoperative surgical planning and training field, for instance, a computational model of the patient based on medical images obtained with non-invasive methods is used to evaluate surgical procedures [1]. The static configuration of internal organs has been modeled in previous work, but the dynamic response of soft tissue, including contact forces between adjacent tissues, was not well characterized. In the automobile engineering field, computational models of passengers have been studied to predict vehicular ride comfort in the early stages of automobile design [2]. Distribution of contact pressure between the seat cushion and the passenger's anatomy have been well validated. However, conventional modeling studies did not focus on the dynamic response of soft tissues inside the passenger's body, thus the relationship between dynamics and subjective comfort are yet to be clarified. The reason for this gap in dynamics modeling can be attributed to the lack of a robust method to quantify it. Therefore, modeling the human body dynamics requires developing a measurement method that can characterize the *in vivo* dynamics of soft tissue.

Ultrasound is a promising imaging modality for observing the *in vivo* dynamic motion and deformation of soft tissue due to its compact form, low cost, high sampling rate, and non-invasive nature. Several techniques using ultrasound imaging have been developed in the field of image-guided surgery to interact with a rapidly moving target such as a beating heart [3]. 3D reconstruction from 2D ultrasound images by actively swiping the ultrasound probe has been also studied for temporally and spatially tracking an object inserted to a body [4].

The ultrasound imaging technologies mentioned above enable the measurement of dynamic motion and deformation of soft tissue. The work presented here combines an ultrasound imaging system with a whole-body vibration exciter. Using this system, the dynamic characteristics of soft tissues can be identified as a frequency response function by associating the observed response with the input vibration. An optical tracker is used to compensate for the vibration-induced motion of the ultrasound probe. In addition to the design of the developed system, initial results of abdominal organs and upper leg are presented in the paper.

2. METHODS

2.1. System Design

The system consists of (1) an ultrasound imaging device, (2) a vibration exciter, and (3) an optical tracker, as shown in Fig. 1. An ultrasound imaging device (Sonos 7500, Philips Healthcare, Andover, MA, USA) was used to take images of soft tissue for recording the dynamic response. A transesophageal endoscopic (TEE) ultrasound probe (Omni III, Philips Healthcare, Andover, MA, USA) was affixed to the surface of the passenger's body. The TEE probe was chosen for its low-profile, reducing inertial loads that can cause the probe to move during excitation, as well as its omnidirectional ultrasound imaging plane. An active seat suspension system (Bose Ride System, Bose Corporation, Framingham, MA, USA), which was originally developed to reduce passen-

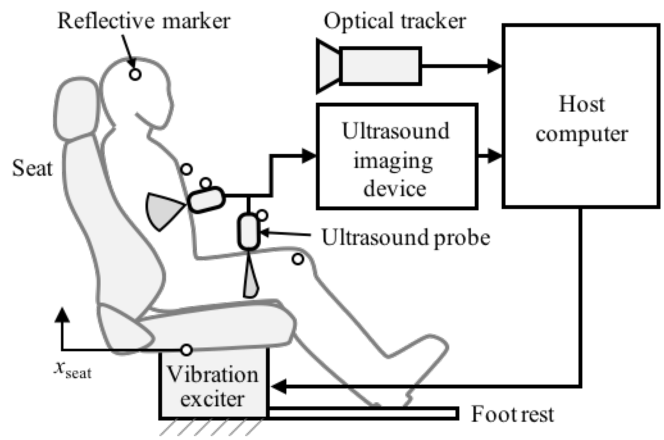

Fig. 1. Setup of the developed system

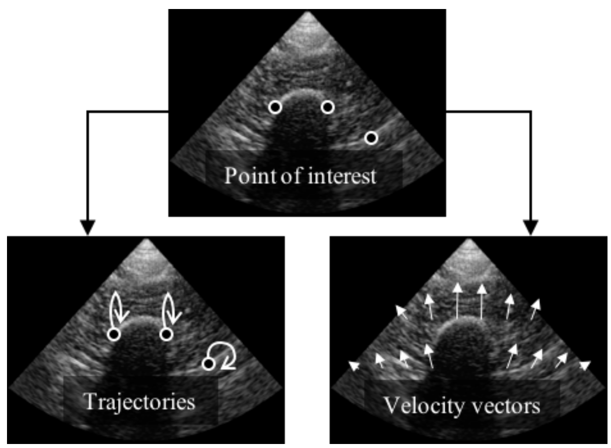

Fig. 2. Image processing pipeline

ger's vibration by counteracting external disturbances, was repurposed as a vibration exciter. Its powerful electromagnetic actuator lends itself well to generating input vibrations that can mimic road conditions. An optical tracker (fusionTrack500, AtracSys GmbH, Switzerland) was used to track the spatial position of reflective markers at a sampling rate of 333 Hz and accuracy of 90 μm. Passive motion of the ultrasound probe, the responses at the surface of passenger's skin, and the vertical seat motion x_{seat} were tracked.

2.2. Experimental Procedure

After attaching the reflective markers, ultrasound images and trajectories of the reflective markers were recorded while the seated subject was exposed to whole-body vibrations. The experimental subject maintained their posture throughout the experiment. In order to temporally align the ultrasound images with the optical tracker data, the ultrasound probe was given a step input both at the beginning and the end of the experiment.

Fig. 2 outlines the image processing pipeline schematically. First, each point of interest (POI) in the ultrasound images was identified with the Shi-Tomasi minimum-eigenvalue algorithm. Second, the POIs were tracked by using the Kanade-Lucas-Tomasi feature tracking algorithm, then displacement fields in the ultrasound images were calculated. Velocity fields were also calculated using the Lucas-Kanade optical flow algorithm.

Trajectories of POIs were synchronized with the optical tracker data by associating the trajectory of the POIs with that of the ultrasound probe. Then, identified trajectories were transformed into the world coordinate system by compensating for the passive motion of the ultrasound probe. The vertical component of the transformed trajectory of POI was defined as x_{output}. Relative position and orientation between the ultrasound imaging plane and the reflective markers attached to the ultrasound probe were previously calibrated using the algorithm described in PLUS [5]. Finally, the frequency response function (FRF) of soft tissue, $A(\omega)$, was calculated as a transfer function defined as

$$A(\omega) = \frac{X_{output}(\omega)}{X_{seat}(\omega)} \tag{1}$$

where X is the Fourier transform of x, and ω is a frequency.

2.3. Experimental Conditions

Ultrasound images of both the abdominal organs in the sagittal plane and the upper leg in the transverse plane were acquired to identify dynamics using the developed system.

Two kinds of input signals, sinusoidal and frequency-sweep, were introduced. Frequency of the sinusoidal signal ranged from 1 Hz to 10 Hz at 1 Hz intervals. The frequency of the frequency-sweep continuously ranged from 1 Hz to 10 Hz across a 20-second time span. Two amplitudes, 1 m/s^2 r.m.s. and 2 m/s^2 r.m.s., were employed for each signal type. However, a combination of 2 m/s^2 r.m.s. and 1 Hz was omitted due to the travel limits of the vibration exciter.

One subject participated in the experiment. The subject was asked to have a seat on the vibration exciter with standard posture and maintain the initial posture while the vibrations were induced. Preexperimental training was conducted in advance of the data collection to accustom the subject to the vibrations.

The experimental procedure and condition were approved by the Harvard University Institutional Review Board.

3. RESULTS

Fig. 3 (a) shows a raw ultrasound image of the abdominal organs. Stomach, liver, abdominal muscles, and the surrounding connective tissue - such as omentum - can be seen in the image. The abdominal muscles were recognized as a thick layer separated from other internal organs with a bright curve.

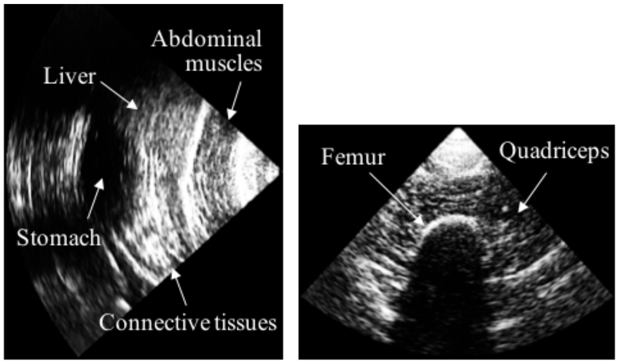

(a) Abdominal organ (b) Upper leg

Fig. 3. Raw ultrasound images

The stomach was observed as a black hollow area surrounded by a bright ellipsoidal perimeter. Fig. 3 (b) shows the upper leg, where the femur and surrounding quadriceps can be seen in the image. Since the ultrasound is mostly reflected at the surface of the bone, only the top edge of the femur was observed as a bright arc.

Fig. 4 shows FRFs for (a) the head, (b) the sternum, and (c) the knee. The responses were observed at the surface of the passenger's skin during the frequency-sweep excitation. These were directly calculated from the optical tracker data. FRFs for (d) the abdominal muscle, (e) the stomach, and (f) the femur are also shown in Fig. 4. These responses acquired with the sinusoidal excitation were extracted from the ultrasound images by using the method described in Section 2. The solid lines represent the response to 1 m/s^2 r.m.s., and the dotted lines represent those to 2 m/s^2 r.m.s. of input level. The curves were interpolated using a cubic spline algorithm.

Fig. 5 shows phase diagrams of tracked POIs and velocity fields at a certain phase for (a) the abdominal organ at 4 Hz and (b) the upper leg at 8 Hz in the condition of 1 m/s^2 r.m.s.. For phase diagrams, the stomach wall and the femur's top edge are shown as examples, respectively.

4. DISCUSSION

Peaks of magnitude and phase delays shown in Fig. 4 suggest that the passenger-seat coupled system has resonance characteristics. However, the resonance frequencies vary with location in the body, implying that the observed resonance characteristics were caused by local structures and mechanical properties in addition to whole-body structure. Since the experimental subject reported that 4 Hz of imparted vibration was the most uncomfortable, it is implied that the resonances at the head, the abdominal muscle, and the stomach can induce the subjective feeling of discomfort.

Correlations between x_{seat} and all x_{output} were high, suggesting that the linear analyses are feasible. However, as shown in Fig. 4, the FRFs depend on the amplitude of the input signal, indicating that the passenger-seat coupled system is essentially nonlinear. In external responses shown in Fig. 4 (a), (b), and (c), higher amplitude causes the resonance frequency and the peak levels of $|A(\omega)|$ to be lower. In con-

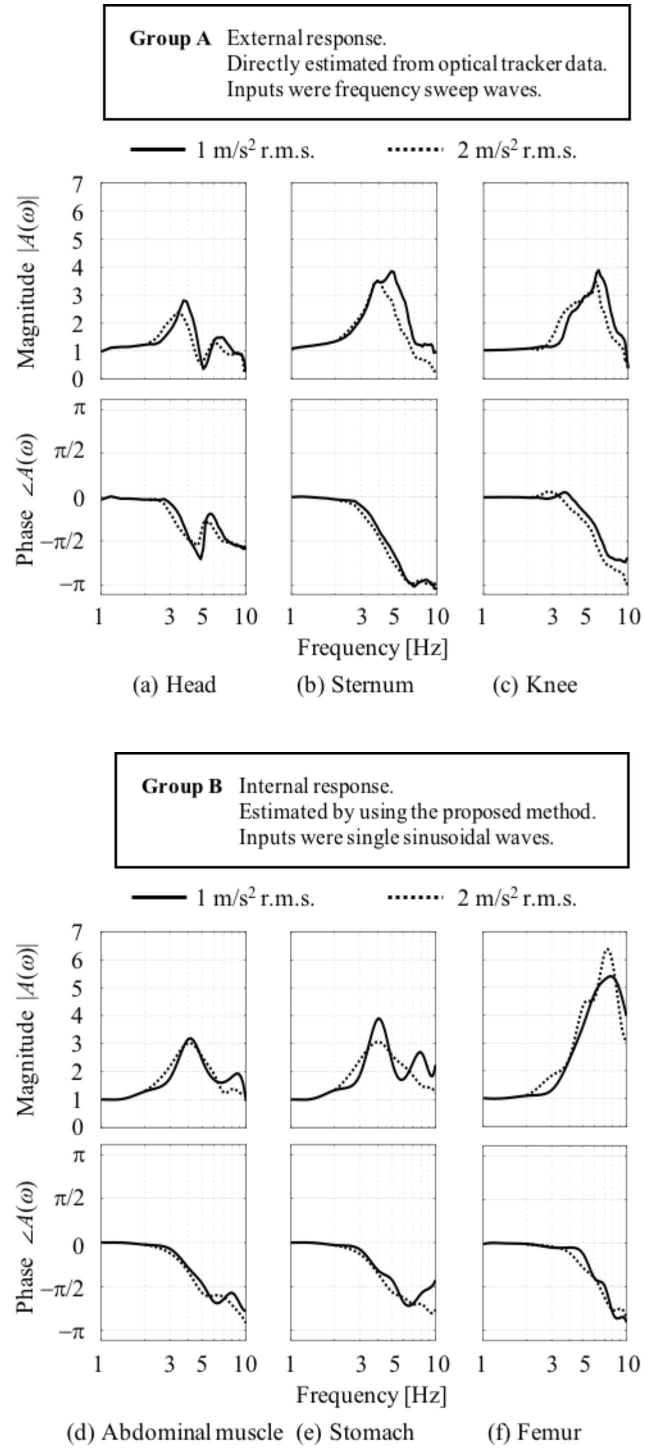

Fig. 4. Frequency response functions

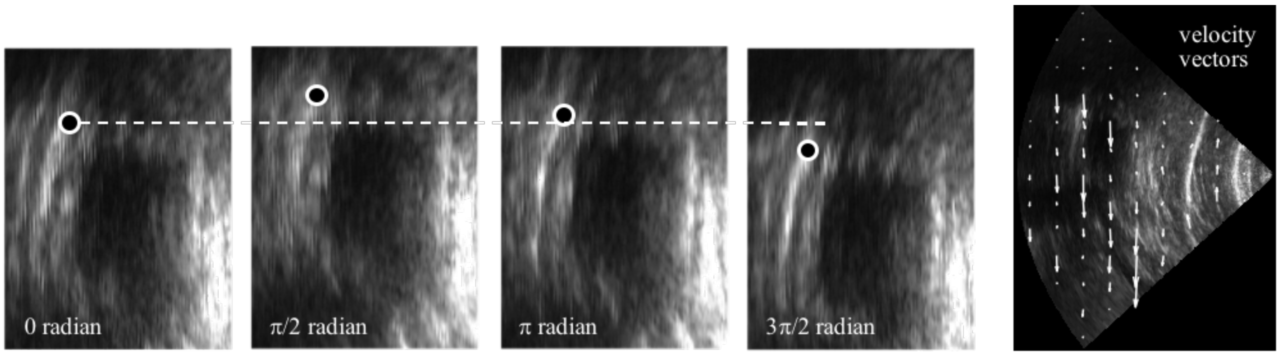

Phase diagram of tracked stomach wall

Velocity field at π radian

(a) Abdominal organ, 4 Hz, 1 m/s^2 r.m.s.

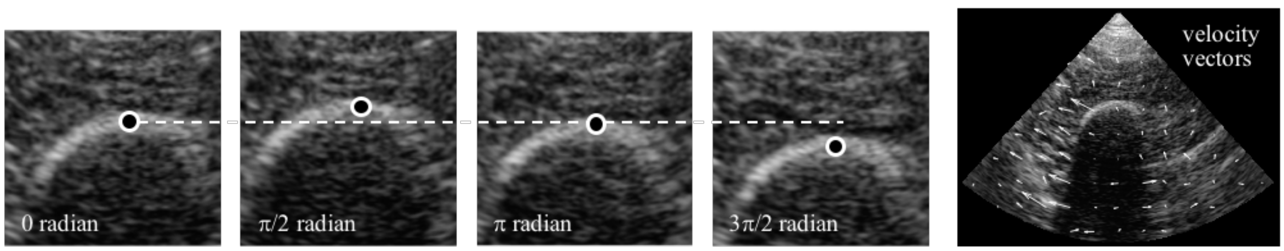

Phase diagram of tracked top edge of femur

Velocity field at $\pi/2$ radian

(b) Upper leg, 8 Hz, 1 m/s^2 r.m.s.

Fig. 5. Phase diagram and velocity fields

trast, no consistent tendency due to the amplitude is observed in the internal responses shown in Fig. 4 (d), (e), and (f). Further experiments with more participants are required to reveal the amplitude dependency and repeatability as well as inter-subject variation.

As shown in the phase diagram in Fig. 5, cyclic vertical vibrations of soft tissue are clearly observed. However, as shown in the velocity fields of (a) the abdominal organs, the direction of velocity of the stomach is shifted from that of the abdominal muscle. Passive motion of the ultrasound probe caused by the imparted vibration can be one reason of the phase difference. However, the difference in dynamics between the abdominal muscle and the stomach can be considered to be dominant to the phase delay between the velocities, because the characterized phase at 4 Hz in FRFs have a difference of approximately $\pi/8$ radian. It can be also considered that the viscoelasticity of the abdominal tissues might cause the phase delay. Moreover, the quadriceps respond not only in the vertical but also the lateral direction as shown in the velocity field in Fig. 5 (b), though only a vertical input was applied. It is revealed that multi-dimensional vibration modes can be observed inside the passenger's body.

Only one point on each tissue was tracked with the Kanade-Lucus-Tomasi feature tracking algorithm in this work for taking a general view of the tissue dynamics. Better understanding about the tissue motion and deformation requires more advanced image processing techniques, such as pattern matching and four-dimensional reconstruction. Several kinds of algorithms based on pattern matching, for instance speckle tracking, are used in echocardiography to evaluate deformation and strain of the heart [6]. It is considered that the pattern matching is essentially applicable to the method presented here instead of the Kanade-Lucus-Tomasi method. However, the fundamental difficulty is the unexpected passive motion of the ultrasound probe caused by the excitation. Advanced 2D image processing methods could potentially improve the precision of the tracking, however, compensation for the shift in the ultrasound imaging plane is still required. Segmentation of the tissues from the 2D ultrasound image and arranging them temporally should be one promising method to identify the soft tissue dynamics. In addition to the temporal arrangement, introducing the spatial arrangement by using further data obtained with other observation points and angles will enable four dimensional reconstruction. The combination of the data obtained from multiple observation points inherently realize the identification of the motion and deformation mode on the soft tissue.

As mentioned in the section 2.2, the relationship between the ultrasound imaging plane and the reflective markers attached to the ultrasound probe was calibrated in advance of the data collection. A rigid phantom was introduced for the calibration, then the resultant error in the calibration was so small that the spatial accuracy of tracked POI is within a couple of pixels in the ultrasound image. The pixel size generally depends on the penetration depth of the ultrasound wave. In the setup of the data collection reported here, the penetration depth was 10 cm, resulting in the spatial accuracy of approximately 0.5 mm. Errors in the feature tracking might worsen the spatial accuracy, however, the ideal accuracy seems to be sufficient to calculate the FRF under 10 Hz of frequency with the input levels introduced here. High correlations between the input signals and the output responses also support the sufficiency of the accuracy because it proves that corresponding responses of soft tissue to input excitation were successfully measured.

5. CONCLUSIONS

A tissue dynamics characterization system comprising an ultrasound imaging system, a vibration exciter, and an optical tracker is presented. The system can identify *in vivo* soft tissue dynamics as a frequency response function. Dynamics of soft tissue in abdominal organs and upper leg were characterized using the developed system, and shown to be different from those observed at the skin surface.

Four dimensional reconstruction of motion and deformation shapes will be conducted in future work. The identified shapes of soft tissue, including boundaries with adjacent tissues, will be utilized for developing a computational human body model and for estimating contact forces between tissues by utilizing inverse finite element analysis.

6. ACKNOWLEDGEMENT

This work was supported by Toyota Motor North America, Inc.

7. REFERENCES

[1] M.A. Scherer and D.A. Geller, "New Preoperative Images, Surgical Planning, and Navigation," *Imaging and Visualization in The Modern Operating Room: A Comprehensive Guide for Physicians*, pp. 205–214, 2015.

[2] A. Siefert, "Occupant Comfort - A Mixture of Joint Angles, Seat Pressure and Tissue Loads," in *Proceedings of SAE 2016 World Congress*. SAE, April 2016, SAE Technical Paper 2016-01-1438.

[3] S.G. Yuen, N.V. Vasilyev, P.J. del Nido, and R.D. Howe, "Robotic Tissue Tracking for Beating Heart Mitral Valve Surgery," *Medical Image Analysis*, vol. 17, no. 8, pp. 1236–1242, December 2013.

[4] P.M. Loschak, L.J. Brattain, and R.D. Howe, "Algorithms for Automatically Pointing Ultrasound Imaging Catheters," *IEEE Transactions on Robotics*, vol. 33, no. 1, pp. 81–91, February 2017.

[5] A. Lasso, T. Heffter, A. Rankin, C. Pinter, T. Ungi, and G. Fichtinger, "PLUS: Open-source toolkit for ultrasound-guided intervention systems," *IEEE Trans. Biomed. Eng.*, vol. 61, no. 10, pp. 2527–2537, October 2014.

[6] S. Sitia, L. Tomasoni, and M. Turiel, "Speckle tracking echocardiography: A new approach to myocardial function," *World Journal of Cardiology*, vol. 2, no. 1, pp. 1–5, January 2010.